Full Paper Transactions, SMiRT 28
Toronto, Canada, August 10-15, 2025

EXPERIMENTAL DEMONSTRATION OF CANDU ANNULUS SPACER LOAD REDISTRIBUTION MECHANISM

Eric Tulk[1], Tom Gallacher[2], Winnie Lau[3], Shawn Lowe[4], Liane Catibog[5]

[1] Senior Engineer, Kinectrics, Inc, Toronto, Canada (eric.tulk@kinectrics.com)
[2] Scientist, Kinectrics Inc., Toronto, Canada (tom.gallacher@kinectrics.com)
[3] Technical Engineer, Ontario Power Generation, Pickering, Canada (winnie.lau@opg.com)
[4] Technical Engineer, Ontario Power Generation, Pickering, Canada (shawn.lowe@opg.com)
[5] Assistant Analyst, Kinectrics Inc., Toronto, Canada (liane.catibog@kinectrics.com)

ABSTRACT

Canadian Deuterium Uranium (CANDU) reactors comprise horizontal pressure tubes containing fuel and coolant inside a calandria containing a heavy water moderator. Coil spring spacers are used to separate the otherwise hot pressure tube from the cooler calandria tube. These Inconel X-750 spacers embrittle due to neutron irradiation and the loss of ductility reduces the load bearing capacity of the spacer. Fitness-for-service is assessed by comparing average coil capacities from flat platen 'crush tests' of ex-service spacers, and the bounding coil load in the reactor configuration from finite element modelling. As load on a reactor spacer is increased, the relatively flexible calandria tube elastically deforms and more coils become engaged to share the increased load. A test programme to experimentally show this spacer load redistribution mechanism was completed and used to validate modelling. The test results confirmed that that the modelling approaches used in fitness-for-service were reliable.

BACKGROUND

Canadian Deuterium Uranium (CANDU) reactors comprise horizontal pressure tubes containing fuel and coolant inside a calandria vessel containing a heavy water moderator. The hot Zr-2.5Nb pressure tubes are each surrounded by an insulating annulus inside cooler Zircaloy calandria tubes. The calandria tube is nominally 132 mm diameter with 1.4 mm wall thickness and is more flexible than the pressure tube. Four annulus spacers are installed around the pressure tube at intervals along the ~6 m length of the channel to separate the pressure tube from the calandria tube. Spacers are coiled wire helical springs which must have adequate structural strength to carry interaction loads imposed between the pressure tube and calandria tube. One type of design installed in some reactors uses an 'optimized' Inconel X-750 spacer design that is tight fitting around the pressure tube, as shown in Figure 1.

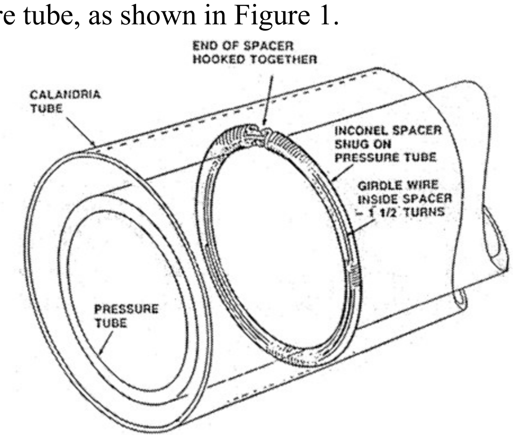

Figure 1. A fuel channel annulus spacer installed on a pressure tube inside a calandria tube.

Inconel X-750 is known to become embrittled under CANDU fuel channel neutron irradiation, and the loss of ductility reduces the load bearing capacity of the spacer component. The material degradation is primarily associated with the segregation of helium bubbles to grain boundaries, Griffiths (2013). Degradation is monitored by periodic material surveillance including mechanical 'crush' tests of ex-service spacers. The measured coil failure loads are used with predictive engineering models to assess ongoing fitness-for-service based on the in-service applied loads, Lau (2019). 3D FEA has demonstrated that downward loads from the pressure tube initially cause spacer coils at the 6 o'clock position to engage against the calandria tube. The calandria tube deforms slightly in response to this loading, and more spacer coils circumferentially outwards from 6 o'clock contact the calandria tube. The total applied load is continually redistributed over those coils in contact. As the load on the spacer is increased, an increasing number of spacer coils near the bottom of the channel physically support the load transfer to the calandria tube. This coil load redistribution mechanism lowers the maximum individual radial coil load which is evaluated in fitness-for-service assessments, compared to if loads remained concentrated over few coils only.

To provide additional confidence in component integrity, the extent to which this load redistribution mechanism occurs was experimentally validated. Due to the small component size, complex system geometry, and lack of clearances for instrumentation access within the annular gap, it was not feasible to directly measure or infer the individual spacer coil loads using conventional methods such as load cells, strain gauges, or digital image correlation. Therefore, a bespoke testing apparatus was commissioned and a novel method to measure spacer coil engagement was developed. The measurements of spacer coil engagement were used to quantify some key aspects of the spacer coil load redistribution and to provide additional semi-quantitative observations which could be compared to FEA results. This paper describes the experiments which were used to validate the modelled structural mechanics of this unique but critical CANDU reactor component.

APPARATUS

A test apparatus was designed and constructed to demonstrate load distribution mechanism, Figure 2. A tight-fitting reactor grade Inconel X-750 spacer was located at the midplane of a 'Pressure Tube Surrogate'. The diameter of the PT surrogate at the spacer position matched the as-manufactured outside diameter of a CANDU pressure tube. The PT surrogate included a hinge on one end and an interface with an electromechanical load frame on the other. The PT surrogate was balanced using a counterweight such that the deadweight load at the spacer position was <10 lbf. This arrangement was such that when a downwards load is applied by the load frame, the load at the spacer position is the sum of the deadweight and the effect of the remotely applied load.

A 2000 mm long reactor grade calandria tube section was installed around the PT surrogate and spacer and simply supported using chocks at each end. This arrangement was necessary because it allowed the application of spacer loads via the PT surrogate while maintaining the full cross section (i.e. no holes for loading access in the calandria tube) and a substantial length of calandria tube about the spacer. With the application of the downwards 'spacer load', the calandria tube is permitted to elastically bend axially and change cross-section (ovalise). This calandria tube arrangement was seen as a suitable analog to a reactor fuel channel, where spacers are nominally 1000 mm apart.

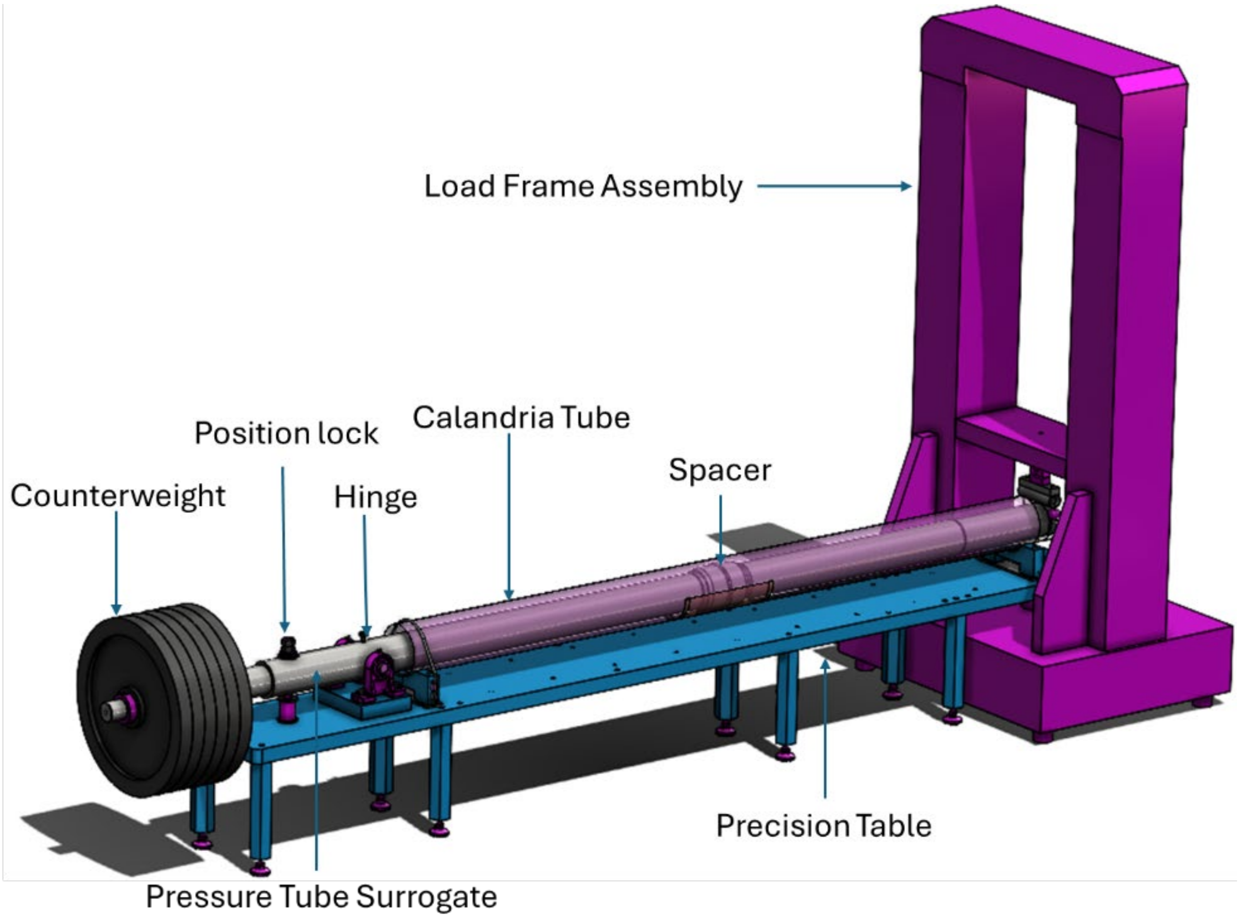

Figure 2. Schematic of Spacer Load Distribution Test Rig.

Prior to the installation, the load applied at the spacer position, was measured using a button type load cell. This was used to calibrate the required load frame to achieve the required 'spacer load' of 50, 100, 200, 300, 400, 500, 600, 700, and 800 lbf. The estimated uncertainty of the spacer load was <3 lbf. The range of loads used in the test included loads well above and below in-service spacer operational load levels to provide a more complete data-set for evaluating the mechanism.

To infer the load in the individual spacer coils, pressure sensitive contact paper was used. Contact paper contains small ink bubbles in the material that burst under applied pressure. The papers are available in a range of different pressure ranges. There is a 'pressure floor', below which the ink will not burst, and a 'pressure ceiling', where the ink bursting effect saturates. The intensity of the colour increases over the range between the pressure floor and ceiling. Sheets of contact paper were affixed to a 3d printed part matched to the ID of the calandria tube, and a carbon fibre rod. This arrangement allowed the contact paper to be easily shifted near the spacer position remotely from the ends of the calandria tube. The ultimate outcome of the paper is that it records the *maximum* pressure applied to a region of the paper. The rig calibration and careful test procedures ensured that there was no risk of spacers being loaded above the intended levels, and thus precluded false positive coil indications associated with any overshoot loads. A contact paper assembly is shown in Figure 3.

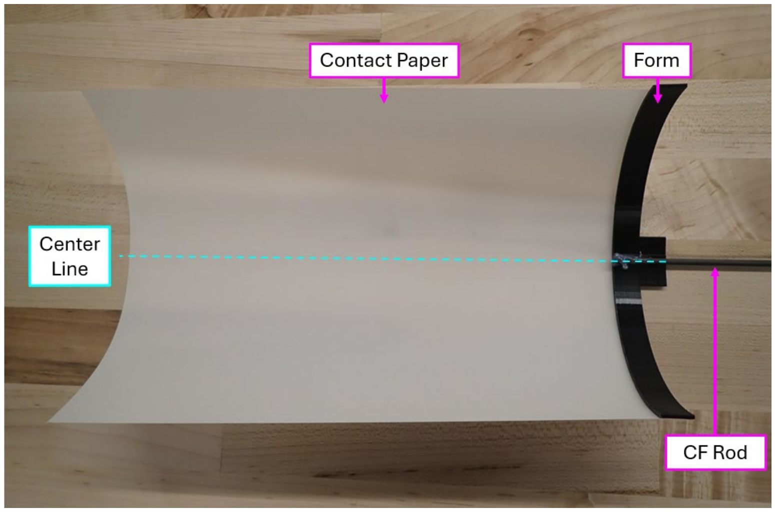

Figure 3. Contact Paper Assembly.

Physical measurements on how the calandria tube deformed due to spacer loads were collected to support the model validation effort. The deformation was monitored using strain gauges, an LVDT, and other physical measurements. An LVDT monitoring the vertical position of the calandria tube was located at the 6 o'clock position immediately below the spacer. Biaxial strain gauge rosettes measuring axial and circumferential strain were located along the 6 and 12 o'clock outer fibres at the spacer position, and one and two inch positions away from one side of the spacer. The 6 o'clock gauge at the spacer position was shifted to 5 o'clock to avoid interference with the LVDT. Physical measurements of the 3-9 o'clock diameter, and the height of the 12 o'clock position of the calandria tube were collected while the calandria tube was loaded using a height gauge and calliper. Taken together, the LVDT and physical measurements are suitable to describe the calandria tube flexure (i.e. from bending), and its cross section ovalisation. The strain gauge rosettes show the evolution of the strain field in the vicinity of the spacer.

EXPERIMENTAL RESULTS

On a typical load application, the PT surrogate was supported by a strop attached to the load frame, and a small (few mm) annular gap was present between the spacer and calandria tube at the 6 o'clock position. The contact paper assembly was then installed at an appropriate position beneath the spacer, sitting down on the calandria tube inner surface. The load frame crosshead displaced downwards, first allowing the deadweight load of the PT surrogate to push on the spacer, and then gradually applying a prescribed downwards load. The load was held for 10 seconds, and then the frame returned to its starting position with the aforementioned annular gap. The contact paper was then either removed or shifted for the subsequent load application.

For the nine load levels tested (50-100-200-300-400-500-600-700-800 lbf), a minimum of three impressions for each of three contact paper pressure range were collected. These measurements confirmed excellent repeatability of the trials. Contact paper with pressure ranges of 350 to 1,400 psi (low), 1,400 to 7,100 psi (medium), and 7100 to 18,500 psi (high) were used. Multiple contact paper ranges were used to help discern the relative coil loads across the spacer.

Figure 4 shows a zoom of a contact paper impression corresponding to a spacer load of 400 lbf. This shows a series of red indications where the spacer coils loaded against the calandria tube activated the contact paper. A mosaic showing the contact paper impressions for all load levels on the same contact paper type is included in Figure 5. The impressions from the lowest applied load are shown in the top row, and the effect of increasing the applied load progressively bringing more coils into contact is seen in each subsequent row. The coil impressions appear similar across most coil positions but decrease in size towards the periphery of the spacer. This clearly shows that, with increasing spacer load, both the number of coils in contact (judged by the number of independent coils counted on the impression paper), as well as the local coil loads (judged by the intensity of the impression colour), increased with increasing load.

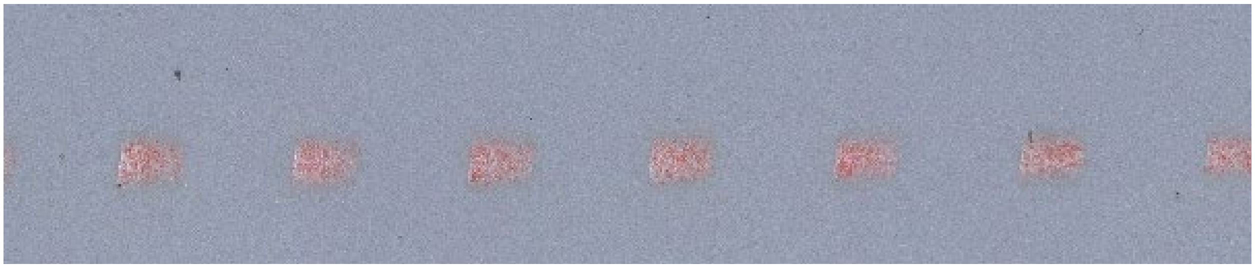

Figure 4. Zoom of typical contact paper impressions on ‘High’ contact paper at 400 lbf spacer load.

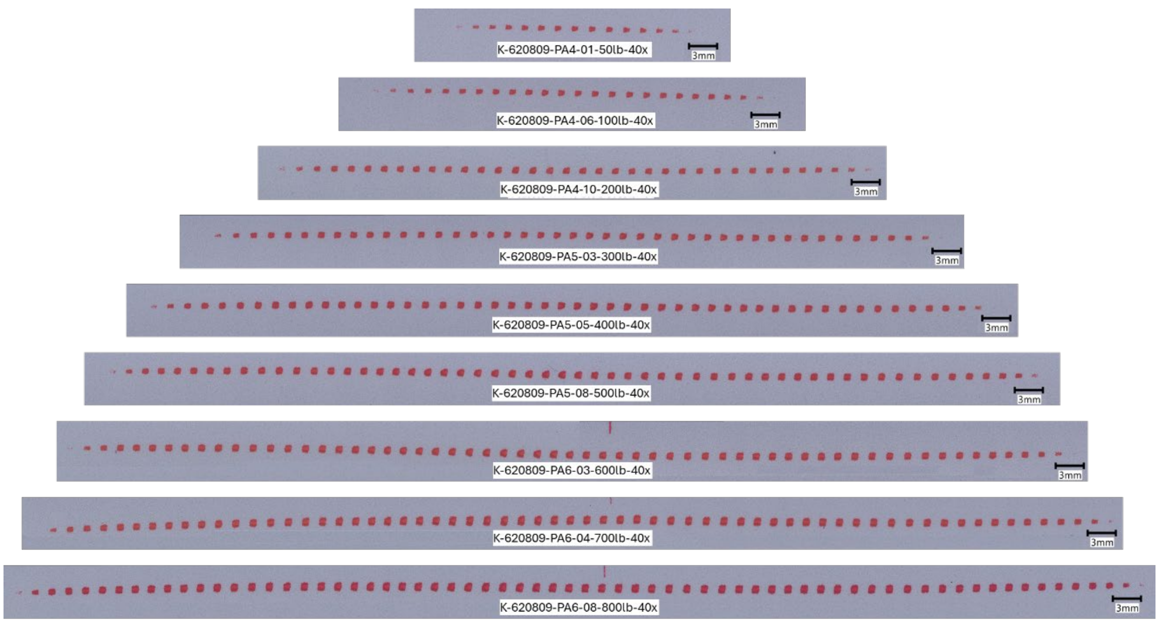

Figure 5. Mosaic showing contact paper impression results for ‘Medium’ contact paper from 50 lbf to 800 lbf of spacer load.

Separate testing of a section of spacer coils loaded between two flat platens was used to estimate the applied coil loads required to activate the pressure paper to various intensity levels. Results suggested that the ‘High’ threshold contact paper would not record coil contact at loads below approximately 10 N/coil, whereas the more sensitive paper types had saturated indications at lower load levels. Comparison of experimental measurements of the same spacer load using different pressure paper types could therefore be used to differentiate regions of high and low spacer coil loads.

The calandria tube was shown to clearly sag with increasing spacer load. The calandria tube cross section also ovalised during load application, with the diameter shrinking at 3 and 9 o’clock, and expanding at 6 and 12 o’clock. This ovalisation occurs because the larger diameter, thin walled calandria tube elastically flexes to conform to the shape of the smaller diameter pressure tube and spacer. The general deformation measurements are shown in Figure 6.

The strain gauges along the 12 o'clock position of the calandria tube showed strain fields typical of bending, which was unsurprising as there was no local strain field expected associated with the spacer, which was contacting at 6 o'clock. The strain gauges on the bottom of the calandria tube showed much higher strain magnitudes and what was clearly the sum of section bending strains plus the local strain field associated with the spacer pushing on the calandria tube. The strain development in the calandria tube is shown in Figure 6.

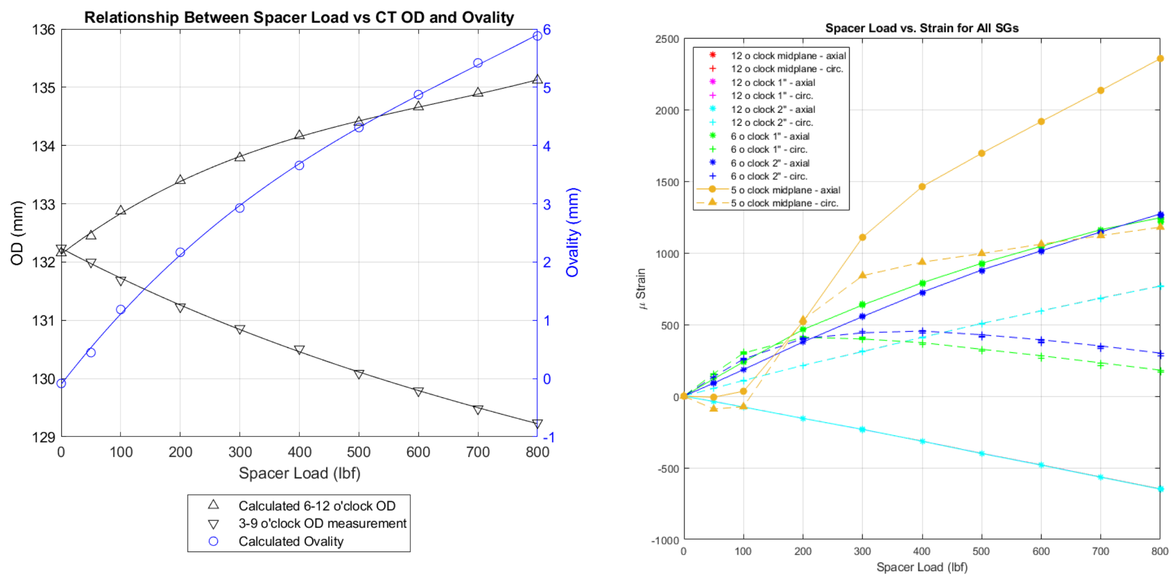

Figure 6. Deformation and strain of calandria tube due to spacer loads.

COMPARISON AGAINST MODELLING

A detailed, 3-dimensional finite-element model of the CANDU fuel channel has been developed in ANSYS and includes channel-specific ageing effects including creep deformation of the pressure tube and calandria tube. This model has been applied to assess various operating scenarios, including to determine the loads on spacers and on individual spacer coils. This model was adapted to represent the experimental test configuration by removing some reactor components, the irradiation effects, and adjusting the material properties to simulate the ambient temperature laboratory environment. The remaining components of a calandria tube section, pressure tube section and single spacer were modelled using the measured dimensions of the tested components, and by setting boundary condition restraints to represent the support at either end of the tested calandria tube, and to apply loads to the spacer through the pressure tube section. The finite-element mesh and contact settings were retained from the fuel channel model. The model applied the same increasing spacer loads as were tested, and the spacer coil loads and calandria tube deformation and strains were extracted at steps throughout the simulation for comparison against experimental results. The deformed shape of the half-symmetry model is shown in the left panel of Figure 7.

The vertical deflection of the bottom of the calandria tube at the loaded spacer location was confirmed to match experimental measurements, which provided confidence that boundary conditions at the ends of the calandria tube appropriately capture the tested configuration. Spacer coil to calandria tube contact is shown in the right panel of Figure 7, where the helical spacer coils can be seen to violate the symmetric boundary condition. If there were *n* coils in contact in the half-model, then $2n$ - 1 coils were assumed to be representative for comparison to the experimental results. Such a comparison is shown in Figure 8, where there is a stepwise increase in the number of modelled coils in contact with the calandria tube (since coils are either counted as in contact or not in contact). The model results followed a realistic general trend of increasing spacer coil engagement under increasing applied vertical load, but under-estimated the measured number of coils in contact over the entire loading range. This means that the model concentrated applied loads over fewer coils at the bottom of the channel than was realistic.

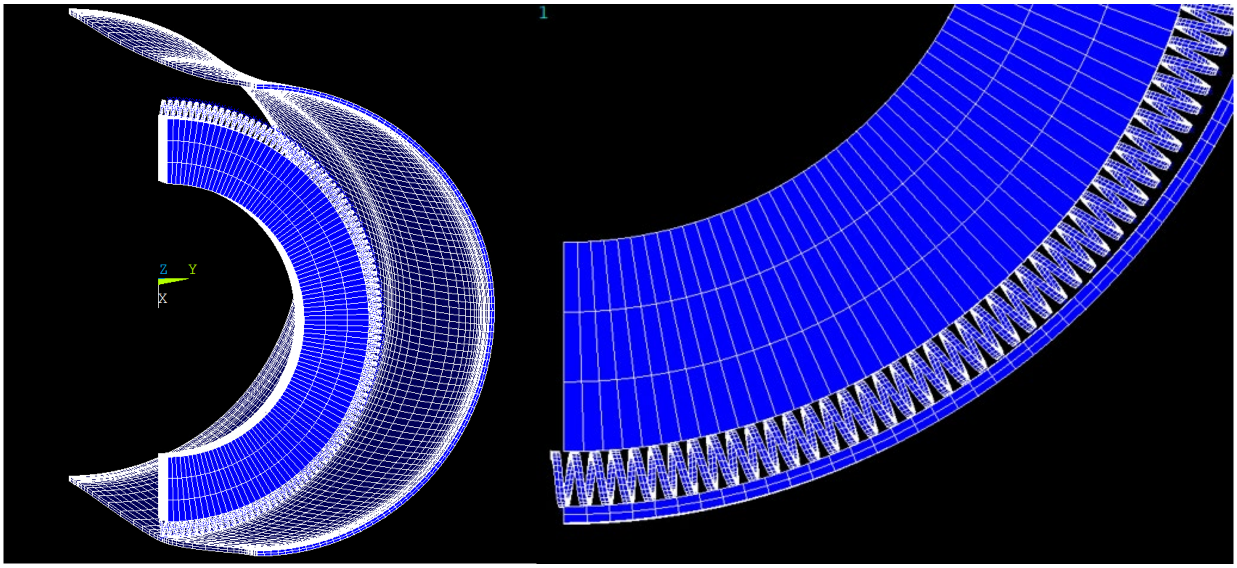

Figure 7. Deformed shape of finite-element model due to spacer loads (left), and detail of spacer to calandria tube contact (right).

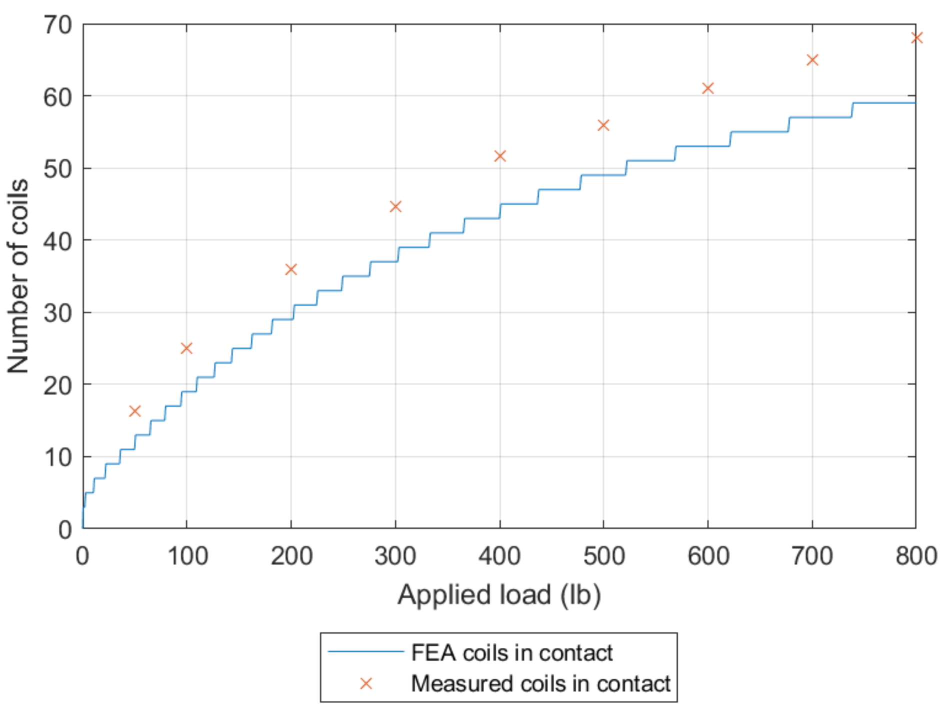

Figure 8. Comparison of the number of coils in contact with the calandria tube from the FEA and measured using pressure paper in the experiment.

Using the different threshold pressure paper levels, it was possible to compare the modelled and measured coil load distributions in more granularity. By considering only coils loaded above certain levels, which were known to only activate the most robust paper type, or to leave darker or larger marks on the pressure paper, the relative individual coil loads may be inferred. Both the experiments and model results show that while the individual coil loads across most of the spacer appear similarly loaded, the individual coil loads decrease on the periphery of contacting coils.

The underlying cause of the model under-prediction of coil engagement was investigated. In both the model and the experiment, as the spacer engages against the bottom portion of the inner surface of the calandria tube, there was an increase in the calandria tube vertical diameter, and a corresponding decrease to the horizontal diameter as the sides pull inwards in response. The measurements of this ovalisation are shown in the left panel of Figure 6. Although the model followed a realistic trend, it under-predicted the extent of this deformation. It was shown that the less-ovalised, more-circular cross section calandria tube resulted in fewer coils being loaded than was realistic. Comparison of simulated and measured strains confirmed that the modelled calandria tube section was circumferentially stiffer than the tested component. Sensitivity studies where this was resolved resulted in improved comparisons against the experiment than shown in Figure 8, where more calandria tube ovalisation promoted increased spacer coil engagement. It was confirmed that greater coil engagement resulted in a decreased peak coil load, and this demonstrated that the 'baseline' model of the experiment as well as the model used for reactor fitness-for-service assessments conservatively over-predicted the maximum spacer coil load.

CONCLUSIONS

- A test rig was developed to study the coil load distribution mechanism in Inconel X-750 CANDU fuel channel spacers. The test rig allowed the realistic elastic bending and ovalisation of a calandria tube section beneath a loaded spacer.
- Testing showed that increasing the spacer load resulted in both an increased number of coils supporting the load, and an increased individual coil load.
- The deformation measurements in the vicinity of the spacer showed reasonable bending deformation of the calandria tube section, the ovalisation of the calandria tube cross-section, and also the development of a local strain field around the spacer.
- A 3-dimensional finite element model of the fuel channel was adapted to represent the test rig. A comparison between the model and experimental results validated the spacer coil load redistribution mechanism, but showed that the model slightly under-estimated the extent of increasing coil engagement under spacer loading, resulting in conservative calculations of the maximum coil loads.
- This validation provided confidence in the fundamental pressure tube to spacer to calandria tube load transfer mechanism used in fuel channel fitness-for-service assessments.

REFERENCES

M. Griffiths, G.A. Bickel, S.A. Donohue, P. Feenstra, C.D. Judge, D. Poff, L. Walters, M.D. Wright L. Greenwood, and F.A. Garner, (2013), *Degradation of Ni-Alloy Components in CANDU Reactor Cores*, AECL Conference Paper CW-127000-CONF-007, Revision 0.

W. Lau, D. Scarth, and P. Doddihal, P. (2019), *Inconel X-750 Spacer Fitness-for-Service*, Proceedings of the ASME 2019 Pressure Vessels & Piping Conference, PVP2019-93943.